In Situ Effects of Mutations of the Extrinsic Cytochrome c_{550} of Photosystem II in *Synechocystis* sp. PCC6803†

Zhaoliang Li,[#] Heather Andrews,[#] Julian J. Eaton-Rye,[‡] and Robert L. Burnap*,[#]

Department of Microbiology and Molecular Genetics, Oklahoma State University, Stillwater, Oklahoma 74078, and Department of Biochemistry, University of Otago, P. O. Box 56, Dunedin, New Zealand

Received June 25, 2004; Revised Manuscript Received August 23, 2004

ABSTRACT: The H_2O oxidizing domain of the cyanobacterial photosystem II (PSII) complex contains a low potential, c-type cytochrome termed c_{550} that is essential for the in vivo stability of the PSII complex. A mutant lacking cytochrome c_{550} (Δ*psbV*) in *Synechocystis* sp. PCC6803 has been further analyzed together with a construct in which the distal axial heme iron ligand, histidine 92, has been substituted with a methionine (C550−H92M). Heme staining of SDS−PAGE showed that the C550−H92M mutation did not disturb the accumulation and heme-binding properties of the cytochrome. In Δ*psbV* cells, the number of charge separating PSII centers was estimated to be 56% of the wild type, but of the existing centers, 33% lacked photooxidizable Mn ions. C550−H92M did not discernibly affect the intrinsic PSII electron-transfer kinetics compared to the wild type nor did it exhibit a significant fraction of centers lacking photooxidizable Mn; however, the number of charge separating PSII centers in mutant cells was 69% of the wild type. C550−H92M lost photoautotrophic growth ability in the absence of Ca^{2+}, but its growth was not affected by depletion of Cl^-, which differs from Δ*psbV*. Taken together, the results suggest that in the absence of cytochrome c_{550} electron transfer on the donor side is retarded perhaps at the level of Y_z to $P680^+$ transfer, the heme ligand. His92 is not absolutely required for assembly of functional PSII centers; however, replacement by methionine prevents normal accumulation of PSII centers in the thylakoid membranes and alters the Ca^{2+} requirement of PSII. The results are discussed in terms of current understanding of the Ca^{2+} site of PSII.

Photosystem II (PSII)[1] catalyzes the light-driven reduction of plastoquinone using electrons extracted from water via the oxygen-yielding H_2O oxidation reaction (for reviews on PSII, see refs *1*−*4*). A c-type cytochrome, cytochrome c_{550} (cyt c_{550}), is intimately associated with the H_2O oxidation domain of the PSII complex in cyanobacteria and nongreen algae (*5*). Several lines of convincing evidence show that cyt c_{550} is involved in the integrity and stability of PSII complex (*6*−*13*) consistent with its extensive contacts with intrinsic domains as well as with 12 kDa and manganese-stabilizing proteins (MSPs) observed in the current X-ray crystal structure models of the cyanobacterial complex (*14*−*16*).

Although associated with the membrane-bound PSII complex, cyt c_{550} is a water-soluble monoheme cytochrome and exhibits striking structural similarities to other c-type cytochromes, including cytochrome c_6 (also known as cytochrome c_{553}), which carries electrons from the cytochrome b_6/f complex to photosystem I in cyanobacteria and eukaryotic algae. Despite the structural similarities, cyt c_{550} has a much lower midpoint redox potential as compared to the other c-type cytochromes (*17*−*20*). The structurally similar cyt c_6 has a midpoint potential of +325 mV, whereas cyt c_{550} has a midpoint potential of approximately −250 mV. The actual value of heme redox potential of cyt c_{550} in vivo can be modulated by three major factors: the nature of the heme axial ligands, the solvent exposure of the heme, and the protein environment around the heme-binding site (for analysis, see ref *21*). For example, when methionine−histidine heme ligation of cyt c_{550} from *Thiobacillus versutus* was changed to lysine−histidine heme ligation, the redox potential of the mutant shifted −329mV (*22*), and when the solvent water was excluded from the heme-binding site, a shift of +150 mV was observed (*20*). The unusually low midpoint potential of cyt c_{550} is partly attributable to the bis-histidyl axial ligation of the heme iron (*18*, *20*, *21*). Another component of the low potential can be attributed to the comparatively large area of solvent exposure of the heme edge including the propionate moiety observed in the crystal structure (*19*, *23*). The magnitude of this contribution of solvent exposure to the low potential is estimated to be 150 mV as deduced from the difference in midpoint potential of cyt c_{550} measured in solution −260 mV (*18*) as compared to −108 mV as measured by square wave cyclic voltammetry with the protein adsorbed to the graphite electrode surface

† This work was funded by the National Science Foundation (MCB-01323556 to R.L.B.).

* Corresponding author; phone: 405-744-7445; fax: 405-744-6790; e-mail: burnap@biochem.okstate.edu.

[#] Oklahoma State University.

[‡] University of Otago.

[1] Abbreviations: PSII, photosystem II; DCBQ, 2,6-dichloro-*p*-benzoquinone; cyt c_{550}, cytochrome c_{550}, an extrinsic protein of photosystem II complex encoded by psbV; EDTA, (ethylenedinitrilo)tetraacetic acid; DM, dodecyl maltoside; Hepes, 4-(2-hydroxyethyl)-1-piperazineethanesulfonic acid; MES, 2-(4-morpholino)-ethane sulfonic acid; TES, *N*-tris-(hydroxymethyl) methyl-2-amino ethane sulfonic acid; TMBZ, 3,3′,5,5′-tetramethylbenzidine; WOC, H_2O oxidation complex.

10.1021/bi0486738 CCC: $27.50
Published on Web 10/16/2004

(*20*). Concordantly, the midpoint of the cytochrome is −80 mV as measured when the cytochrome bound to the PSII complex, where the otherwise exposed heme edge is buried within the protein−protein binding interface (*24*).

The function of cytochrome c_{550} has remained controversial. Krogmann originally proposed that the function of cyt c_{550} may be related to anaerobic disposal of electrons from carbohydrate reserves to sustain an organism overcoming prolonged dark and anaerobic conditions (*25*). Other proposed functions for cyt c_{550} include accepting electrons from ferredoxin during the oxidation of NADPH and in cyclic photophosphorylation (*26*). These assignments seem to be contradicted by the clear physical association with the H_2O oxidation domain of the PSII complex. However, the very low midpoint potential of the cytochrome adjacent to the strongly positive operating potential of the H_2O oxidation begs the question as to what function, if any, the heme moiety has. Information on the function of cyt c_{550} in PSII was obtained from the cyt c_{550} deletion mutant (Δ*psbV*) and from biochemical depletion/reconstitution studies. Cells of the Δ*psbV* mutant contain half of the PSII centers found in wild type, but are capable of growing photoautotrophically albeit at a reduced rate (*10*, *27*). However, autotrophic growth requires higher levels of Ca^{2+} and Cl^- to satisfy the PSII requirement for these ions, much like mutants lacking the MSP. And like the MSP-less mutants, the cyt c_{550} deletion mutant rapidly loses O_2-evolving activity in the dark, whereas the lost activity can be subsequently restored by the process of photoactivation (*27*−*30*). Biochemical reconstitution experiments have shown that cyt c_{550} alone was able to restore only about 10−11% of oxygen-evolving activity of isolated PSII complex in the absence of the other extrinsic proteins. Addition of MSP alone restored approximately half the activity. However, activity approaching the level of maximal reconstitution is obtained when cyt c_{550} is added in conjunction with MSP, demonstrating the importance of both proteins acting in concert for maintaining the integrity of the H_2O oxidation complex (*7*, *31*). Taken together, the results indicate that cyt c_{550} has an important structural role, but do not answer the question whether the heme moiety has a redox function related to the operation or protection of PSII (*32*).

Here the sixth position axial ligand of cyt c_{550} in *Synechocystis* sp. PCC6803, histidine 92, was mutagenized to a methionine, emulating typical c-type cytochromes with a more positive midpoint potential. In this initial investigation, the mutant strain, C550−H92M, was analyzed and compared with the Δ*psbV* and wild type.

MATERIALS AND METHODS

Construction of Plasmid pPSBV and Site-Directed Mutagenesis. Growth and manipulation of the glucose-tolerant strain of *Synechocystis* sp. PCC6803 was conducted according to established procedures (*33*). Molecular genetic techniques followed standard techniques (*34*). The *Synechocystis* sp. PCC6803 *psbV* gene was amplified from chromosomal by PCR (Turbo *Pfu* polymerase, Stratagene). The oligonucleotide 5′ GCG CGG TAC CGA CCG ATT CC 3′ was used as the forward primer, which introduced a *KpnI* site (underlined), and the oligonucleotide 5′ GGC GAG CTC GCG CTT ACG ATA ATC GTG GC 3′ was used as the reverse primer, which introduced a *SacI* site (underlined). The amplified PCR product was inserted into the *KpnI* and *SacI* sites of the plasmid pBS SK$^-$; the plasmid pPSBV was created by inserting a 1.1 kb kanamycin resistance cassette from pRL446 at the *XbaI* site, which located at stop codon of psbV gene. The primers 5′ GAC TAT TCG GAG CTC **ATG** CCC AAT ATT TCC CGT CCC 3′ and 5′ GGG ACG GGA AAT ATT GGG **CAT** GAG CTC CGA ATA GTC 3′ were used to create the mutant pPSBVH92M, and a *SacI* site was introduced (underlined). Mutagenesis was performed by using the QuickChange Site-Directed Mutagenesis kit (Stratagene). Plasmids pPSBV and pPSBVH92M were used to transform Δ*psbV*, and the transformants were selected and propagated on BG-11 plates supplemented with 20 μM atrazine, 5 mM glucose and 5 g L^{-1} (initially) or 50 g L^{-1} (final platings) kanamycin. The desired mutation was confirmed by both digesting with *SacI* and sequencing the mutagenized plasmid and colony PCR products. The strain of Δ*psbV* transformed with plasmid pPSBV was used as a control and designated as wild type hereafter.

Preparation of O_2-Evolving Membranes and Analysis of S-State Decay. Isolation of O_2-evolving membranes was performed with modifications of previously described procedures (*35*, *36*). Measurements of the kinetics of S-state decay was performed using a bare platinum electrode as previously described (*37*).

Quantification of PSII and Measurements of Fluorescence Kinetics. Measurements of variable fluorescence yields were performed using a Walz PAM 101 chlorophyll fluorometer (Heinz Walz GmbH, Effeltrich, Germany). Cells in late logarithmic phase of growth were harvested by centrifugation. After being washed with HN buffer (10 mM Hepes, pH 7.0, 30 mM NaCl), the cells were resuspended in HN buffer at a final concentration of 50 μg of Chl mL^{-1}, and then the cells were kept under dim light on the shaker at 150 rpm before being used for experiments. Estimation of the concentration of charge-separating PSII centers was performed essentially as described previously (*38*, *39*). Measurement of chlorophyll fluorescence decay was performed essentially as in ref *39*. A 3-mL cell suspension at 3 μg of Chl mL^{-1} was incubated in darkness for 5 min before measuring pulses were switched on at 1.6 kHz and a train of actinic 30 flashes was given at 5 Hz beginning 100 ms later in the presence of 50 μM of DCMU.

Other Procedures. Maximal rates of O_2 evolution were determined polarographically at 30 °C using a Clark-type electrode at a final chlorophyll concentration of 6.25 μg mL^{-1} as described previously (*37*). Samples were resuspended in HN buffer supplemented with 0.75 mM DCBQ and 2 mM potassium ferricyanide. The chlorophyll a concentration was measured in methanol extracts according to ref *40*: using the extinction coefficient at 665.2 nm of 79.24 mL mg^{-1} cm^{-1}. SDS−PAGE was performed on a 12% polyacrylamide separation gel containing 6 M urea. Cyt c_{550} was detected on the basis of its heme-centered peroxidase activity using TMBZ (3,3′,5,5′-tetramethylbenzidine) as previously described procedures (*11*, *31*).

RESULTS

Construction of Cytochrome c_{550} His92 → Met Axial Ligand Substitution Mutant. The sixth position ligand to the

heme iron of cyanobacterial cytochrome c_{550} is histidine 92.[1] Together with histidine 41, it provides a bis-histidyl (bis-His) axial coordination for the heme. This contrasts with other c-type cytochromes, which typically have Met-His axial heme coordination. This difference in axial coordination is thought to account, in part, for the considerably more negative midpoint potentials of the bis-His c-type cytochromes compared to the Met-His coordinated c-type cytochromes (*18*, *20*, *21*). The function of cytochrome c_{550} in cyanobacterial PSII remains unknown. If its function depends on the low midpoint potential of its heme, then conversion of the axial heme ligation to Met−His could impair its function. Therefore, a plasmid vector, pPSBV, was constructed to facilitate the site-directed mutagenesis of the His92 axial ligand of cytochrome c_{550} in *Synechocystis* sp. PCC6803 (see Materials and Methods). The ligand replacement mutation was constructed in the parent vector pPSBV, which was then used to transform a *Synechocystis* recipient strain, ΔpsbV, which entirely lacks the *psbV* gene encoding cyt c_{550} using established techniques (*11*, *33*, *41*). The resultant strain of *Synechocystis*, C550−H92M, expresses only the mutant form of the cytochrome possessing the His → Met ligand replacement. To facilitate the screening for the mutation, a *SacI* site was also introduced within the *psbV* coding sequence as a silent mutation adjacent to the targeted His codon (see Materials and Methods) and the desired mutation was confirmed by restriction digesting with *SacI* and sequencing. The control strain possesses a wild-type copy of *psbV* with a kanamycin-resistance cassette located downstream of the *psbV* gene at the *XbaI* site. Figure 1A, which shows the profile of PCR products of *psbV* gene carrying a kanamycin-resistance cassette digested by *SacI*, confirms that the mutant sequence has been introduced. As expected, wild-type PCR product (1.96 kb) could not be digested by *SacI*, while the C550−H92M PCR product gave two bands, 1.55 kb and 407 bp, respectively, upon digestion with *SacI*. DNA sequencing of the PCR products was performed to verify that the engineered base changes were present in the transformant and to make sure that unintended mutations were not also incorporated into the mutant (data not shown).

Substitution of Axial His92 by Met Does Not Affect Heme Attachment in Cyt·c_{550}. To investigate whether the H92M mutation affects expression of the protein and the covalent attachment of the heme moiety, the cellular lysates from C550−H92M and wild type were analyzed by SDS−PAGE followed by heme-staining with TMBZ while using the Δ*psbV* strain as a negative control. All samples, except Δ*psbV*, showed equivalent TMBZ-staining intensities corresponding to the cyt c_{550} electrophoretic band (Figure 1B). This indicated that the axial ligand substitution by Met did not impair *psbV* gene expression and had no discernible effect upon the maturation of the cytochrome, which involves the cleavage of the signal peptide and the formation of a covalent thioether linkage between the heme moiety and the apoprotein. We also explored the binding ability for cyt c_{550} and MSP to membranes in C550−H92M using previously established methods (*42*−*44*). In these experiments, total cell lysates from mutant and control cells were centrifugally separated into membrane and soluble fractions and analyzed for MSP and c-type cytochrome content. Low concentrations of the nonionic detergent, dodecyl maltoside, were added to promote the release of unbound and nonspecifically bound

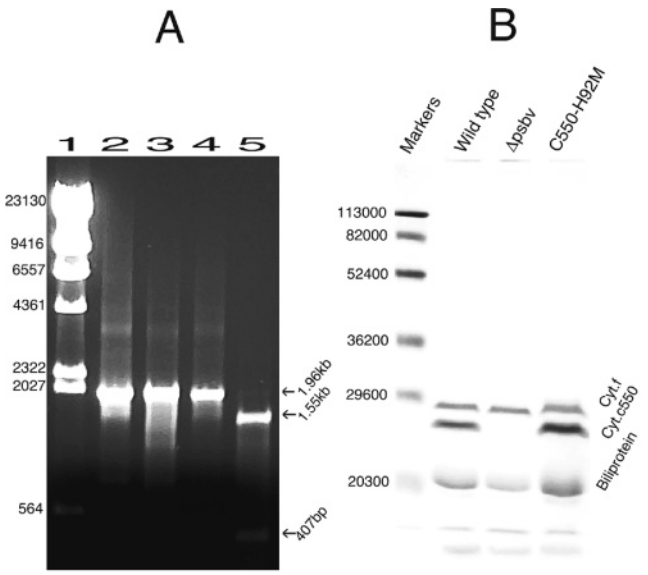

FIGURE 1: (A) PCR was applied to amplify the flanking *psbV* gene with a kanamycin resistance cassette at the *XbaI* site. Lane 1: marker, λ DNA/*HindIII*; lane 2: wild type, undigested; lane 3: wild type, digested; lane 4: C550−H92M, undigested; lane 5: C550−H92M, digested. As expected, wild-type PCR product could not be digested by *SacI*, while C550−H92M PCR product gave two bands, 1.55 kb and 407 bp, respectively, with *SacI*. (B) Heme-staining of the lysate with TMBZ. Cells were disrupted according to ref *44* and samples equivalent to 1 μg of chlorophyll were loaded in each lane. Two individual wild type and C550−H92M lysate preparations were analyzed. Wild type was *psbV* gene carrying kanamycin resistance cassette at the *XbaI* site, which had no effect on its expression and PSII function. All samples except Δ*psbV* showed the TMBZ-staining specific cytochrome c_{550} band, suggesting the axial ligand substitution by methionine had no effect on *psbV* gene expression and heme binding.

proteins associated with membrane fragments and vesicles. C550−H92M exhibited no detectable change in the association of these extrinsic proteins with the membrane fraction compared to that of wild type indicating that the ligand substitution mutation did not cause a large change in c_{550} binding affinity for its site on the PSII reaction center (data not shown). However, this binding assay is inherently crude, and nonspecific binding and incomplete removal of unbound proteins cannot be entirely discounted. Taken together, the results indicate that the presence of the axial ligand mutation does not markedly affect the synthesis and assembly to its location in the PSII complex.

Substitution of Axial Histidine 92 by Met Increases the PSII Calcium Requirement. To explore potential effects of the mutation on the function of the PSII complex, growth experiments were performed. The effects of calcium and chloride on the growth of mutant C550−H92M and wild type were examined in the calcium- or chloride-limiting BG-11, respectively. For the calcium-limiting BG-11, the usual 0.24 mM $CaCl_2$ was replaced with 0.48 mM NaCl, and for chloride-limiting BG-11, $MnCl_2$, and $CaCl_2$ were replaced by equivalent amounts of $MnSO_4$ and $Ca(NO_3)_2$ respectively. Under these conditions, the wild type is able to grow using the trace concentrations of these ions that are residual in the medium, whereas PSII mutants with reduced affinity for these ions are unable to grow (*9*, *27*, *39*, *45*, *46*). The rescue of growth upon addition of glucose suggests that the altered ion requirement is localized at PSII. C550−H92M lost photoautotrophic growth ability in the absence of calcium

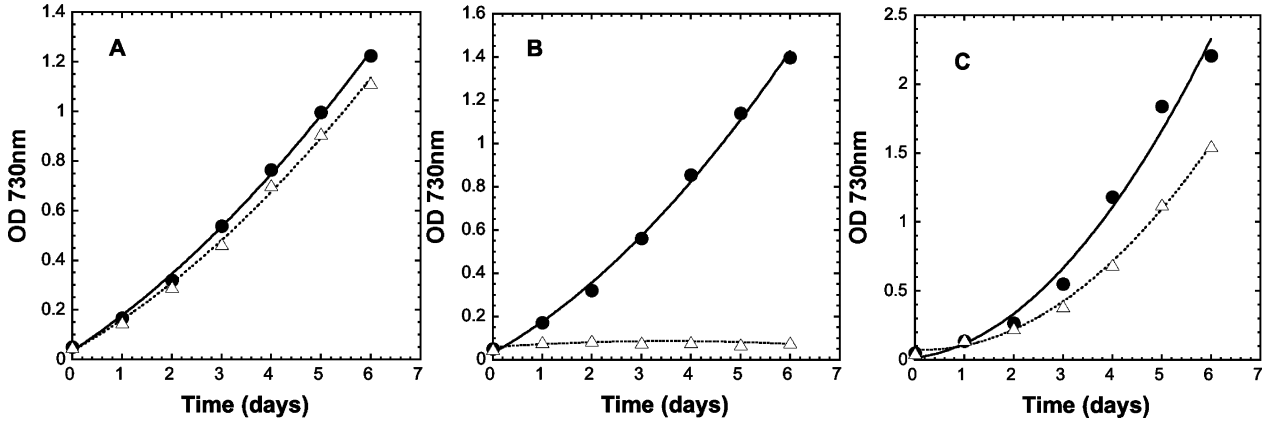

FIGURE 2: Growth characteristics of cyt c_{550} mutant, C550−H92M, as measured by the optical density at 730 nm. Photoautotrophic growth of C550−H92M in the chloride-limiting BG-11 media (A) and in the calcium-limiting BG-11 media (B). Panel C shows mixotrophic growth characteristics of C550−H92M in the calcium-limiting BG-11 media supplemented with 5 mM glucose. Wild type, closed circles; C550−H92M, open triangles.

Table 1: Characterization of cyt c_{550} Mutants of *Cyanobacterium Synechocystis* sp. PCC6803[a]

strain	O_2 evolution[b] μmol of O_2· (mg of Chl)$^{-1}$·h^{-1}(%)	O_2 evolution[c] μmol of O_2· (mg of Chl)$^{-1}$·h^{-1}(%)	O_2 evolution[d] μmol of O_2· (mg of Chl)$^{-1}$·h^{-1}(%)	PSII content[e] $(F_{max} - F_0)/F_0$ (%)
wild type	650(100)	630(100)	660(100)	0.50(100)
C550−H92M	449(69)	359(57)	455(69)	0.35(69)
Δ*psbV*	202(31)	34(5.4)	178(27)	0.28(56)

[a] All the data was the average of three or more measurements. [b] Oxygen evolution was measured at a chlorophyll concentration of 6.25 μg mL^{-1} in HN buffer (10 mM Hepes, 30 mM NaCl, pH 7.2) with the addition of 750 μM DCBQ and 2 mM $K_3Fe(CN)_6$. [c,d] Oxygen evolution was measured after 6 h dark incubation and after giving 10 min continuous light to the samples of 6 h in the dark, respectively. [e] Measurements were taken in the presence of 20 mM hydroxylamine and 40 μM DCMU according to Nixon and Diner (*38*) and Chu et al. (*39*). A PAM 101 chlorophyll fluorometer with a PAM 103 triggering attachment (Walz Inc., Germany) was used in this experiment.

(Figure 2B), but was able to grow, albeit, at a slightly lower rate than that of wild type in the absence of chloride (Figure 2A). However, glucose restored the growth of C550−H92M, although at a slower rate than that of wild type in the absence of calcium (Figure 2C). This is different in comparison to Δ*psbV*, which lost photoautotrophic growth ability in the absence of calcium or chloride (*11*, *27*). The results that both C550−H92M and Δ*psbV* require standard calcium concentrations to support their photoautotrophic growth imply that both the deletion and axial ligand mutations reduce the affinity of the calcium binding to its binding site in PSII. The fact that alteration of the Cl^- requirement of PSII is observed in the mutant completely lacking cyt c_{550}, but not in the site-directed H92M axial mutant, is consistent with the previous conclusion that the H92M form of the cytochrome remains bound to the PSII complex.

PSII Concentration and Oxygen Evolution Activity. Measurements of the relative concentration of PSII centers according to variable fluorescence and the maximal rates of O_2 evolution using the artificial electron acceptor DCBQ are shown for the mutant and control cells in Table 1. Both the C550−H92M and Δ*psbV* strains exhibit decreased maximal rates of steady-state O_2 evolution as supported by the artificial electron acceptor. Maximal rates of steady-state O_2 evolution paralleled the estimated concentration of PSII for C550−H92M, but not Δ*psbV*, which displays a disproportionately lower rate of O_2 evolution than the estimated concentration of PSII (31 vs 56%). This may be due to the presence of a fraction of 33% of PSII centers in Δ*psbV* lacking photooxidizable Mn ions (see below). This fraction of PSII centers is capable of charge separation but incapable of O_2 evolution.

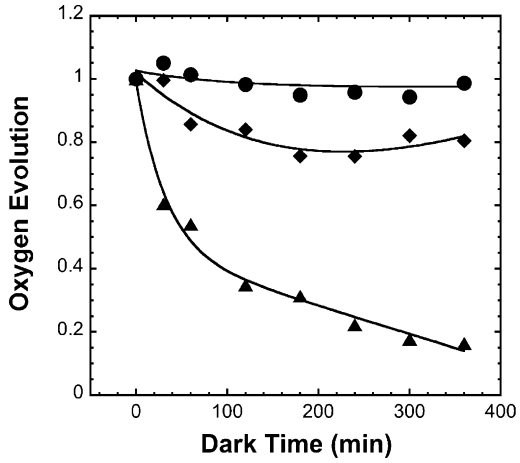

FIGURE 3: Decay of oxygen evolution activity in the dark. Cells were resuspended to a Chl concentration of 100 μg/mL and maintained in the dark with gentle agitation on a rotary shaker. Aliquots were withdrawn at the indicated times, and rates of maximal oxygen evolution were measured and expressed as a fraction of the rates determined prior to the onset of the dark period. Wild type, circles; C550−H92M, diamonds, Δ*psbV*, triangles.

The other alternative, namely, that *psbV* deletion mutation results in a slower enzymatic turnover of PSII, is less likely since earlier results suggest that the slow-down is rather small and less than the acceptor side turnover rates (*27*).

The stability of O_2-evolving activity in whole cells incubated in the dark is shown in Figure 3. The wild-type oxygen evolution activity was essentially unchanged after 6 h incubation in the dark, whereas C550−H92M and Δ*psbV* showed decreases of 20 and 83%, respectively, following

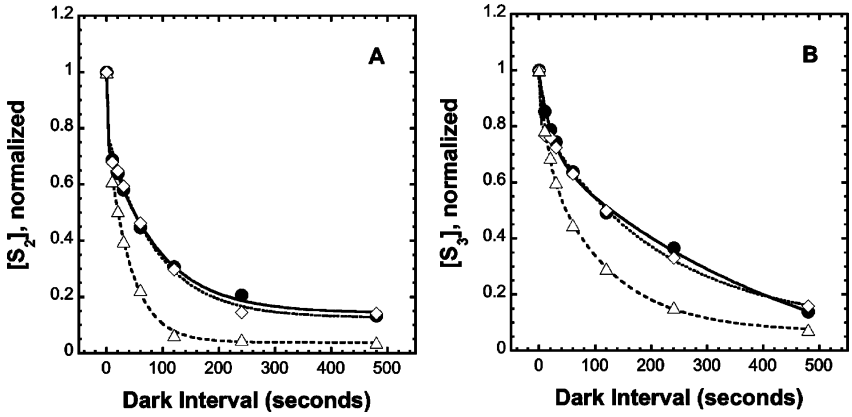

FIGURE 4: S-state decay. Decay of the S_2-state (A) and decay of the S_3-state (B) in thylakoid membranes of the wild type, closed circles; C550−H92M, open diamonds; Δ*psbV*, open triangles. Measurements of the lifetimes of the S_2-state were performed by recording the amplitude of O_2 yield on the third flash under conditions varying the time interval between the first and second flashes. Measurement of the lifetime of the S_3-state in each of the different strains was performed by recording the amplitude of O_2 yield on the third flash under conditions varying the time interval between the second and third flashes (*38*, *56*, *81*).

the same period of dark incubation. Brief illumination of these samples restored activities to levels approaching their original preincubation values (Table 1). The results obtained with Δ*psbV* are consistent with previous observations (*27*). Previous studies have demonstrated that the absence or defective binding of the extrinsic proteins causes the relatively facile loss of the active site metal ions (*47*−*51*) and loss of O_2 evolution in vivo (*9*, *28*−*30*, *39*, *52*), and it has been assumed that the light-dependent restoration of O_2 evolution activity is due to the rebinding of Mn ions lost during the dark incubation period (*28*−*30*, *42*). Therefore, the loss of activity in the C550−H92M is interpreted to indicate that the mutation distorts the cytochrome c_{550} structure in a way that perturbs the $(Mn)_4$ binding site, but not as severely as the complete loss of the protein.

S-State Decay. Figure 4 shows the results of measurements of the dark stability of the S_2- and S_3-states performed using double-flash techniques with isolated thylakoid membranes (*37*, *38*, *53*, *54*). Samples that are allowed to incubate in the dark for 10 min relax to an S-state distribution corresponding to 25% of the PSII centers in the S_0-state and 75% in the S_1-state of the H_2O oxidation complex (data not shown). The dark incubated samples may then be advanced to the S_2- or S_3-states by application of either one or two xenon flashes, respectively. These higher S-states gradually decay corresponding to the rereduction of the H_2O-splitting enzyme by electrons from the acceptor side of the PSII complex from the redox active tyrosine, Y_D, on the donor side of the complex, and ill-defined "endogenous donors" (*45*, *55*, *56*). Accelerated S-state decays were observed in the Δ*psbV* mutant, while C550−H92M displayed kinetics similar to those of wild type (Figure 4). Accelerated S-state decays in Δ*psbV* may indicate that the deletion of cyt c_{550} alters the redox properties of the recombining charge pairs affecting their reactivity toward each other according to previous considerations of this type of reaction (*54*, *55*, *57*, *58*). Since little or no change is observed in the forward electron-transfer rates from Q_A^- to Q_B as assayed by fluorescence (not shown, but see below), changes in the S-state decay kinetics are probably the result of changes on the donor side of the PSII complex. Therefore, the accelerated S-state decays may be due to a more positive S_2/S_1 and S_3/S_2 redox potential of the $(Mn)_4$ cluster or a more negative $Y_D/Y_D^\bullet$ couple resulting in a larger redox gap between the donor and acceptor sides in these mutants. Alternatively, the loss of cyt c_{550} may render the Mn and/or substrate H_2O intermediates more accessible to the solvent, allowing the exchange of partially oxidized substrate H_2O with solvent H_2O returning the enzyme to the S_1-state.

Table 2: Charge Recombination Kinetics between Q_A^- and Oxidized PSII Electron Donors in Cyt·c_{550} Mutants of *Synechocystis* sp. PCC6803

	kinetics of Q_A^- decay after a single flash[a]					
	component 1		component 2		component 3	
strain	(%)	$t_{1/2}$ (ms)	(%)	$t_{1/2}$ (ms)	(%)	$t_{1/2}$ (ms)
wild type	10	13	48	310	42	1150
C550−H92M	12	8	45	310	43	1210
Δ*psbV*	26	7	18	520	56	1510

[a] Kinetics of Q_A^- decay after a single flash was measured in the presence of 50 μM DCMU and analyzed assuming three exponentially decaying components according to Chu et al. (*39*). The relative amplitude (%) and the rate constant of each component.

Fluorescence Characterization of the psbV Mutants. Variable chlorophyll *a* fluorescence yield is proportional to the concentration of Q_A^- in *Synechocystis* sp. PCC6803 (*38*, *45*). In the absence of DCMU, Q_A^- reoxidation occurs mainly via forward electron transfer to either the quinone (Q_B) or semiquinone (Q_B^-) form of the exchangeable plastoquinone. C550−H92M and Δ*psbV* exhibited unchanged forward electron transfer compared to the wild type (data not shown) indicating that the cytochrome c_{550} mutations had little or no change in the acceptor side of PSII. In the presence of DCMU, electron transfer is blocked from Q_A^- to Q_B and the reoxidation of Q_A^- occurs mainly via back-reaction to the oxidized state of the primary PSII donor $P680^+$, which is in redox equilibrium with $Y_z^\bullet/Y_z$ and the S_2/S_1-states of the $(Mn)_4$. C550−H92M exhibited fluorescence decay characteristics that were similar compared to wild type; however, Δ*psbV* exhibited significantly slower fluorescence decays (Figure 4A). The slow decay kinetics of Q_A^- reoxidation in the presence of DCMU in the Δ*psbV* mutant likely indicates a lower equilibrium concentration of $P680^+$ due to a more negative midpoint potential of $Y_z^\bullet/Y_z$ and/or S_2/S_1. The

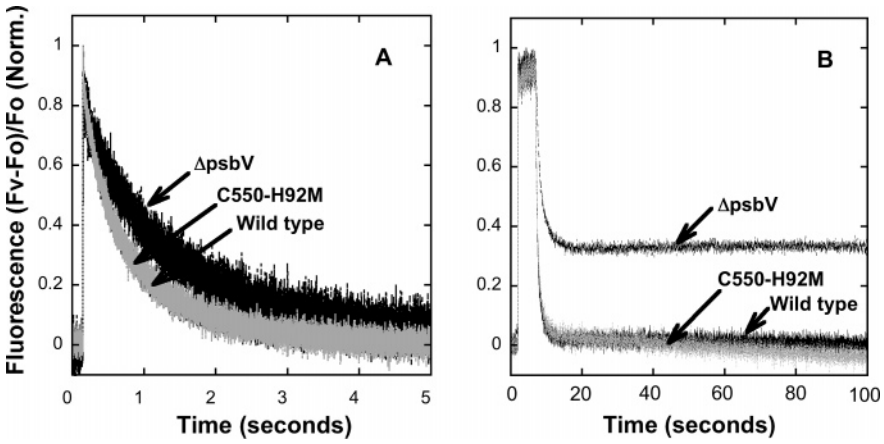

FIGURE 5: Fluorescence characterization of the mutants, C550−H92M and Δ*psbV*. (A) Fluorescence yield kinetics of Q_A^- reoxidation in the presence of DCMU. The charge recombination kinetics of Q_A^- can be measured following a single flash in the presence of 50 μM DCMU and analyzed assuming three exponentially decaying components (see Table 2). (B) Formation and decay of Q_A^- in response to 500 ms continuous saturating illumination in the presence of DCMU. The fraction of photoaccumulated Q_A^- in Δ*psbV* during 500 ms illumination was 33%, reflecting the fraction of PSII centers in Δ*psbV* lack that photooxidizable Mn ions.

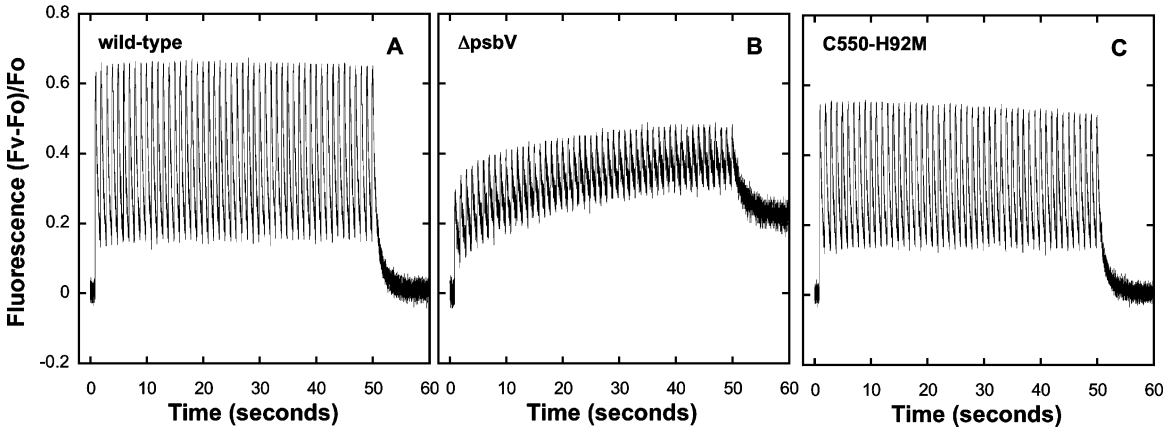

FIGURE 6: Formation of Q_A^- in response to 50 saturating xenon flashes at 1 Hz in the presence of DCMU.

reoxidation kinetics of Q_A^- following a single flash in the presence of DCMU was analyzed assuming three exponentially decaying components corresponding to reduction of different PSII donors (see Table 2).

The fraction of photooxidizable Mn ions in PSII centers can be determined when cells are briefly illuminated in the presence of DCMU (*59*). The fraction of photoaccumulated Q_A^- in Δ*psbV* during 500 ms illumination was 33% (Figure 4B), indicating that approximately 33% of the assembled, charge-separating PSII centers in Δ*psbV* lack photooxidizable Mn ions. Therefore, the overall reduction in PSII oxygen evolving activity in the Δ*psbV* has two components: first, the reduction in the number of assembled reaction centers capable of charge separation, and second, as many of the remaining charge separating centers do not contain a functional manganese cluster.

The characteristics of charge separation were further investigated using fluorescence techniques by following the formation of Q_A^- in response to 50 flashes at 1 Hz in the presence of DCMU; this was also examined to test the efficiency of electron transfer (Figure 6). The lower yield of variable fluorescence followed the first flash in Δ*psbV* and the subsequent gradual accumulation of Q_A^- (Figure 6B) suggests that electron transfer from the WOC to $P680^+$ is slower than in wild type and C550−H92M (Figure 5A,C). Since the addition of hydroxylamine in the assay (performed during quantitation of PSII) restores the fluorescence yield on the first flashes to near wild-type levels, it is likely that the slow-down in $P680^+$ reduction is at the level of $Y_z^\bullet$ reduction by the WOC in the Δ*psbV* mutant. Another interesting observation is that the amplitude of the flash-induced variable fluorescence in C550−H92M progressively declined during the course of the experiment. This phenomenon is only observed in the presence of DCMU, which suggests that charge recombination between the Q_A^- and S_2-state of the $(Mn)_4$ cluster may result in the production of chemical species which react to produce toxic secondary products that are damaging to PSII.

DISCUSSION

The role of extrinsic cyt c_{550} in cyanobacterial PSII oxygen evolution has been explored by deletion of the *psbV* gene and by biochemical depletion−reconstitution experiments (*6*, *8*, *10*, *12*, *27*, *31*, *60*). While a structural role in maintaining the integrity of the H_2O oxidation complex is evident from these studies, an understanding of how the protein modulates the activity of the H_2O oxidation reaction and the significance of the heme group of the cytochrome remain elusive. In the present study, the electron-transfer characteristics of the Δ*psbV* deletion mutant, which entirely lacks the cytochrome, has been analyzed in greater detail than before. Additionally, a new strain, C550−H92M, was constructed in which the

bis-histidyl heme ligation was substituted by a methionine at the sixth position histidine. The C550−H92M mutant described here is the first to explore the role of cyt c_{550} in PSII oxygen evolution by site-directed amino acid substitution mutagenesis.

The C550−H92M substitution mutation does not prevent assembly of the functional PSII complex, although it does decrease the accumulation of PSII in the thylakoid membranes to 69% of the wild type (Table 1). Furthermore, the binding of cyt c_{550} or MSP to the intrinsic domains of PSII was not markedly changed by the C550−H92M substitution mutation. Upon dark incubation, Δ*psbV* was found to rapidly lose oxygen evolution activity, which was consistent with previous results (*27*); however, C550−H92M exhibited only a slight decline in O_2 evolution in comparison to the wild type. These observations are consistent with a rather subtle structural change caused by the H92M mutation. Structural modeling of the cytochrome suggests that an approximately 3.5−4.0 Å deviation in the protein backbone at the substituting Met 92 and/or the heme iron is required to allow coordination of the iron by the methionyl sulfur atom. Experiments are under way to determine if this ligation occurs. Bis-histidine and histidine-methionine are the most common ligation combinations, although other combinations include lysine-histidine, α-amino-histidine, and bis-methionine (*61*−*64*). Among the mutant cytochromes with a substitution of heme-iron axial ligand by histidine, methionine, lysine, or cysteine via semisynthesis or site-directed mutagenesis, some significantly reduced or completely lost bound heme (*63*, *64*), whereas others effectively maintained heme binding with the ligand substitutions (*22*, *62*, *65*−*69*). The cyt c_{550} heme axial ligand change from His to Met in C550−H92M did not affect heme binding because the protein extracts of the strain also showed the TMBZ-staining specific cyt c_{550} band (Figure 1B). This suggests the methionine effectively functions as the sixth heme axial ligand, although further analysis of the isolated protein will be needed to assess this. Usually, the natural c-type hemes with Bis-histidine ligation have lower redox potential in the range of −400 to −100 mV, whereas those with histidine−methionine have higher values in the range of 0 to 400 mV (*70*). Although the midpoint potential of the mutant cytochrome has not been measured in the present study, it is likely that the midpoint potential follows this trend toward positive values.

Consistent with earlier analysis, the mutational loss of cyt c_{550} results in an increased dependence upon Ca^{2+} and Cl^- ions. However, Ca^{2+} deficiency also has a profound impact upon growth of the C550−H92M strain, despite the fact that the expression, maturation, and binding of cyt c_{550} appears largely unaffected by the H92M mutation. Regarding the last point, however, it is also important to note that the binding assay is crude and therefore may not be sensitive enough to reveal a reduction in the binding affinity of cyt c_{550} to the PSII complex. It is likely, based upon the dark deactivation characteristics shown in Figure 3, that some decrease in binding affinity occurs as result of the H92M mutation. Whatever actual changes in binding affinity of cyt c_{550} in the C550−H92M strain, it is clear that the perturbation of cyt c_{550} has a strong effect upon the PSII Ca^{2+} site. Vrettos et al found that the absence of the 17 and 23 kDa proteins causes the free energy of binding (ΔG_B) of cations to the Ca^{2+} site to increase by approximately 2.5 kCal mol^{-1} regardless of the cationic species (*71*). They attribute the decreased affinity of the Ca^{2+} site to an increase in the local dielectric field surrounding the Ca^{2+} site in the absence of the extrinsic proteins due to the closer approach of solvent water. The proximity of polarizable solvent was argued to effectively screen the charge−charge interactions that stabilize the binding of Ca^{2+} to its site within the WOC. Current structural models of the PSII complex indicate that the $(Mn)_4$ is buried under the extrinsic proteins and the C-terminal segment of the D1 protein (*14*, *15*). The removal of cyt c_{550} from the WOC reduces the distance between the solvent-accessible protein surface and the center of the $(Mn)_4$ by approximately 30 Å according to current structural models of the PSII complex and would leave an approximately 10 Å layer of protein covering the $(Mn)_4$. Assuming close proximity of the Ca^{2+} site to the $(Mn)_4$, as with current models, then this difference in solvent proximity could account for a change in Ca^{2+} affinity. On the other hand, the C550−H92M amino acid substitution mutation may not dramatically affect the binding of cyt c_{550}, which would suggest that bulk solvent is not allowed to penetrate in large amounts to sites close to the Ca^{2+} site. If the lowered Ca^{2+} affinity is indeed due to changes in the local dielectric field, then the intrusion of relatively small amounts of solvent into the cyt c_{550}−PSII interface may still be sufficient to yield an energy penalty on Ca^{2+} binding that produces the observed Ca^{2+}-sensitive phenotype. The argument that Ca^{2+} affinity is sensitive to even a relatively small amount of "leakiness" in the protein shield normally provided by the extrinsic proteins has some merit in explaining the diversity of mutations giving rise to the Ca^{2+}-sensitive phenotype since any number of different mutations may cause distortions in protein structure that result in less tightly packed, more solvent permissive, regions of the WOC. The weakened binding of Ca^{2+} upon disturbance of cyt c_{550} binding seems to be reciprocal since perturbation of the Ca^{2+}-binding site by substitution with Sr^{2+} results in weakened binding of cyt c_{550} to isolated PSII particles (*72*).

A puzzling finding is the apparent disparity in the results of the fluorescence decay (Figure 5A) and S-state decay (Figure 4A,B) measurements of the Δ*psbV* mutant. The accelerated decays of S_2 and S_3-states observed in the Δ*psbV* mutant might be interpreted as being due to more positive midpoint potentials of the S_2 and S_3-states of the $(Mn)_4$ cluster. Therefore, the recombination of the $S_2Q_A^-$ state, observed by monitoring the decay of variable fluorescence following a flash in the presence of DCMU, might also be expected to exhibit an accelerated decay. However, there is actually a slowing of fluorescence decay in Δ*psbV* (Figure 5A, Table 2) consistent with a more *negative* midpoint of the S_2-state of the $(Mn)_4$ cluster. Since S-state decays observed on the bare platinum electrode involve recombination from the Q_B site, whereas the fluorescence decay measurements in the presence of DCMU follows recombination from the Q_A site, a possible reason for the discrepancy could be due to an alteration in the Q_B^- site, but not the Q_A site. This, however, seems unlikely on the basis of earlier thermoluminescence (TL) analysis of the mutant (*27*) and the present measurements of fluorescence decay in the absence of DCMU (data not shown, but see above). The TL measurements showed that the peak temperatures of the S_2-Q_A^-, S_2-Q_B^- TL signals increase in parallel indicating that

the effect of cyt c_{550} loss is localized to a change in the donor side and involves shifts to less positive midpoint potentials for $(Mn)_4$ in both the S_2- and S_3-states (*27*). The fluorescence decay measurements in the absence of the inhibitor revealed no differences in forward electron transfer from the Q_A^- to Q_B site, indicating a lack of alteration in the acceptor side upon the loss of cyt c_{550}. The TL and fluorescence results are thus consistent with each other and indicate that the redox potential of the $(Mn)_4$ is less positive. Since a less positive redox potential of the $(Mn)_4$ is expected to result in a slowed S-state decay, yet the decays of both the S_2- and S_3-states measured on the bare platinum electrode are considerably more rapid in Δ*psbV* compared to the wild type (Figure 4), the more rapid S-state decay may have a kinetic, rather than thermodynamic, basis. Therefore, we propose two routes of reduction for the S-states of the $(Mn)_4$: one with a typically observed process of charge recombination between the acceptor side and donor sides with $P680^+$ being an intermediate and the second involving an exogenous electron donor that gains increased access to the $(Mn)_4$ upon the complete removal of cyt c_{550}. This interpretation fits with the rapid dark deactivation of H_2O oxidation activity corresponding to the loss of Mn in Δ*psbV* (Figure 3) since the disassembly of the $(Mn)_4$ involves Mn reduction, presumably by exogeneous reductants. The rapid S-state decay appears to occur in one-electron increments since the centers relax monotonically through the preceding lower S-states to form the usual dark adapted S_0/S_1 ratio of approximately 25/75% (not shown).

There is an apparent decrease in the quantum yield of $S_2Q_A^-$ formation in Δ*psbV* as evident in the multiflash fluorescence experiments (Figure 6B). This result is consistent with increased miss factors for S-state cycling observed with flash O_2 yield experiments using a bare platinum electrode (*27*). Similar observations of submaximal fluorescence yields in response to xenon flashes were made with the D1 a−b loop mutant D1-D59N and D1-D61 mutants under Ca^{2+}-deficient growth conditions (*73*), which also show higher miss factors (*37*). The lower yield of variable fluorescence during flash illumination in Δ*psbV* suggests that electron transfer from the WOC to $P680^+$ is slower than that in wild type and Ca^{2+}-sufficient C550−H92M (Figures 6C and 5D). These observations are in accord with the known perturbation of $Y_z^\bullet$ rereduction and S-state advancement upon Ca^{2+}-depletion. Taken together, the data are consistent with the conclusion that loss or alteration of cyt c_{550} alters the Ca^{2+}-binding site. In this regard, the functional similarities and differences between cyt c_{550} and the 23 kDa extrinsic PSII protein of higher plants and green algae is worth considering: removal of 23 kDa protein has long been known to increase the demand for Ca^{2+} for H_2O oxidation activity (*74*, *75*), and this has been postulated to be due to changes in affinity (*71*). In cyanobacteria, cyt c_{550} has a role in promoting Ca^{2+} binding according to the present and earlier results (*27*). However, some earlier biochemical studies were more equivocal on the issue of the Ca^{2+} requirement of cyanobacterial PSII H_2O oxidation activity and the role of cyt c_{550} in its modulation (*7*, *76*, *77*). Yet, in these cases, rigorous Ca^{2+} depletion methods were not utilized (*7*, *76*) or Ca^{2+} was added back to the O_2 evolution assay buffers (*7*, *77*). If the intimate role of Ca^{2+} in the WOC observed in plants is broadly observed across other oxygenic species including cyanobacteria, as is suggested by the most recent crystal structure model (*14*) and some biochemical studies with *Synechocystis* sp. PCC6803 PSII (*78*), the discrepancies in Ca^{2+} dependencies may be due to incomplete extraction of the ion in those studies reporting only partial dependence of H_2O oxidation activity on Ca^{2+} depletion and readdition.

The most recent structural model of cyanobacterial PSII (*14*) places Ca^{2+} site in close proximity to the D1 carboxy terminal domain with the α-carboxyl group of D1-Ala344 providing one of the Ca^{2+} ligands. Although this specific assignment remains controversial (*79*, *80*), it is likely that Ca^{2+} is in close proximity to the D1 carboxy terminal given its close proximity of PSII Ca^{2+} to the $(Mn)_4$, on one hand, and the likelihood that the carboxy terminus provides Mn ligands, on the other. Both the Kamiya and Ferriera models of the PSII reaction center indicate extensive contacts between the carboxy terminal domain of the D1 protein and cyt c_{550} (*14*, *15*). Given this we suggest that cyt c_{550} modulates the Ca^{2+} site (either through dielectric or direct structural effects) owing to its intimate association with the D1-carboxy terminus.

ACKNOWLEDGMENT

The authors would like to thank Dr. Mario Rivera for help structural modeling of the site-directed cyt c_{550} mutation.

REFERENCES

1. Bricker, T. M., and Ghanotakis, D. F. (1996) Introduction to oxygen evolution and the oxygen-evolving complex in *Oxygenic Photosynthesis: The Light Reactions* (Ort, D., and Yocum, C. F., Eds.) pp 113−136, Kluwer Academic Publishers, Dordrecht, The Netherlands.
2. Britt, R. D., Peloquin, J. M., and Campbell, K. A. (2000) Pulsed and parallel-polarization EPR characterization of the photosystem II oxygen-evolving complex, *Annu. Rev. Biophys. Biomol. Struct. 29*, 463−495.
3. Diner, B. A., and Babcock, G. T. (1996) Structure, dynamics, and energy conversion efficiency in photosystem II in *Oxygenic Photosynthesis: The Light Reactions* (Ort, D., and Yocum, C. F., Eds.) pp 213−247, Kluwer Academic Publishers, Dordrecht, The Netherlands.
4. Debus, R. J. (2000) The polypeptides of photosystem II and their influence on manganotyrosyl-based oxygen evolution in *Metal Ions in Biological Systems* (Sigel, A., and Sigel, H., Eds.) pp 657−711, Marcel Dekker, New York.
5. Kerfeld, C. A., Sawaya, M. R., Bottin, H., Tran, K. T., Sugiura, M., Cascio, D., Desbois, A., Yeates, T. O., Kirilovsky, D., and Boussac, A. (2003) Structural and EPR characterization of the soluble form of cytochrome *c*-550 and of the psbV2 gene product from the cyanobacterium Thermosynechococcus elongatus, *Plant Cell Physiol. 44*, 697−706.
6. Shen, J. R., Ikeuchi, M., and Inoue, Y. (1992) Stoichiometric association of extrinsic cytochrome *c*550 and 12 kDa protein with a highly purified oxygen evolving photosystem II core complex from *Synechococcus vulcanus*, *FEBS Lett. 301*, 145−149.
7. Shen, J.-R., and Inoue, Y. (1993) Binding and functional properties of two new extrinsic components, cytochrome c_{550} and a 12-kDa protein, in cyanobacterial photosystem II, *Biochemistry 32*, 1825−1832.
8. Nishiyama, Y., Hayashi, H., Watanabe, T., and Murata, N. (1994) Photosynthetic oxygen evolution is stabilized by cytochrome *c*550 against heat inactivation in Synechococcus sp. PCC 7002, *Plant Physiol 105*, 1313−1319.
9. Morgan, T. R., Shand, J. A., Clarke, S. M., and Eaton-Rye, J. J. (1998) Specific requirements for cytochrome *c*-550 and the manganese- stabilizing protein in photoautotrophic strains of Synechocystis sp. PCC 6803 with mutations in the domain Gly-351 to Thr-436 of the chlorophyll-binding protein CP47, *Biochemistry 37*, 14437−14449.

10. Shen, J. R., Vermaas, W., and Inoue, Y. (1995) The role of cytochrome *c* 550 as studied through reverse genetics and mutant characterization in Synechocystis sp. PCC 6803, *J. Biol. Chem. 270*, 6901−6907.
11. Shen, J. R., Burnap, R. L., and Inoue, Y. (1995) An independent role of cytochrome *c* 550 in cyanobacterial photosystem, *Biochemistry 34*, 12661−12668.
12. Shen, J. R., Ikeuchi, M., and Inoue, Y. (1997) Analysis of the psbU gene encoding the 12-kDa extrinsic protein of photosystem II and studies on its role by deletion mutagenesis in Synechocystis sp. PCC 6803, *J. Biol. Chem. 272*, 17821−17826.
13. Lakshmi, K. V., Reifler, M. J., Chisholm, D. A., Wang, J. Y., Diner, B. A., and Brudvig, G. W. (2002) Correlation of the cytochrome c_{550} content of cyanobacterial Photosystem II with the EPR properties of the oxygen-evolving complex, *Photosynth. Res. 72*, 175−189.
14. Ferreira, K. N., Iverson, T. M., Maghlaoui, K., Barber, J., and Iwata, S. (2004) Architecture of the photosynthetic oxygen-evolving center, *Science 303*, 1831−1838.
15. Kamiya, N., and Shen, J. R. (2003) Crystal structure of oxygen-evolving photosystem II from Thermosynechococcus vulcanus at 3.7-Å resolution, *Proc. Natl. Acad. Sci. U.S.A. 100*, 98−103.
16. Zouni, A., Witt, H. T., Kern, J., Fromme, P., Krauss, N., Saenger, W., and Orth, P. (2001) Crystal structure of photosystem II from Synechococcus elongatus at 3.8 Å resolution, *Nature 409*, 739−743.
17. Holten, R. W., and Meyers, J. (1963) Cytochromes of a blue-green algae: extraction of a c-type with a strongly negative redox potential, *Science 142*, 234−235.
18. Navarro, J. A., Hervas, M., De la Cerda, B., and De la Rosa, M. A. (1995) Purification and physicochemical properties of the low potential cytochrome C549 from the cyanobacterium Synechocystis sp. PCC 6803, *Arch. Biochem. Biophys. 3186*, 46−52.
19. Sawaya, M. R., Krogmann, D. W., Serag, A., Ho, K. K., Yeates, T. O., and Kerfeld, C. A. (2001) Structures of cytochrome *c*-549 and cytochrome *c*6 from the cyanobacterium Arthrospira maxima, *Biochemistry 40*, 9215−9225.
20. Vrettos, J. S., Reifler, M. J., Kievit, O., Lakshmi, K. V., de Paula, J. C., and Brudvig, G. W. (2001) Factors that determine the unusually low reduction potential of cytochrome c_{550} in cyanobacterial photosystem II, *J. Biol. Inorg. Chem. 6*, 708−716.
21. Mao, J., Hauser, K., and Gunner, M. R. (2003) How cytochromes with different folds control heme redox potentials, *Biochemistry 42*, 9829−9840.
22. Ubbink, M., Campos, A. P., Teixeira, M., Hunt, N. I., Hill, H. A., and Canters, G. W. (1994) Characterization of mutant Met100Lys of cytochrome *c*-550 from Thiobacillus versutus with lysine-histidine heme ligation, *Biochemistry 33*, 10051−10059.
23. Frazao, C., Enguita, F. J., Coelho, R., Sheldrick, G. M., Navarro, J. A., Hervas, M., De la Rosa, M. A., and Carrondo, M. A. (2001) Crystal structure of low-potential cytochrome *c*549 from Synechocystis sp. PCC 6803 at 1.21 Å resolution, *J. Biol. Inorg. Chem. 6*, 324−332.
24. Roncel, M., Boussac, A., Zurita, J. L., Bottin, H., Sugiura, M., Kirilovsky, D., and Ortega, J. M. (2003) Redox properties of the photosystem II cytochromes b559 and c550 in the cyanobacterium Thermosynechococcus elongatus, *J. Biol. Inorg. Chem. 8*, 206−216.
25. Krogmann, D. W. (1991) The low potential cytochrome *c* of cyanobacteria and algae, *Biochim. Biophys. Acta 1058*, 35−37.
26. Kienzel, P., and Peschek, G. (1983) Cytochrome *c*-549: A cofactor of cyclic photophosphorylation in *Anacystis nidulans*? *FEBS Lett. 162*, 76−80.
27. Shen, J. R., Qian, M., Inoue, Y., and Burnap, R. L. (1998) Functional characterization of Synechocystis sp. PCC 6803 delta psbU and delta psbV mutants reveals important roles of cytochrome *c*-550 in cyanobacterial oxygen evolution, *Biochemistry 37*, 1551−1558.
28. Engels, D. H., Lott, A., Schmid, G. H., and Pistorious, E. K. (1994) Inactivation of the water-oxidizing enzyme in manganese stabilizing protein-free cells of the cyanobacteria Synechococcus PCC7942 and Synechocystis PCC6803 during dark incubation and conditions leading to photoactivation, *Photosynth. Res. 42*, 227−244.
29. Burnap, R. L., Qian, M., Al-Khaldi, S., and Pierce, C. (1995) Photoactivation and S-state cycling kinetics in photosystem II mutants in Synechocystis sp. PCC6803 in *Photosynthesis: From Light to Biosphere* (Mathis, P., Ed.) Kluwer Academic Publishers, Dordrecht, The Netherlands.
30. Burnap, R. L., Qian, M., and Pierce, C. (1996) The manganese-stabilizing protein (MSP) of photosystem II modifies the in vivo deactivation and photoactivation kinetics of the H_2O-oxidation complex in *Synechocystis* sp. PCC6803, *Biochemistry 35*, 874−882.
31. Enami, I., Kikuchi, S., Fukuda, T., Ohta, H., and Shen, J. R. (1998) Binding and functional properties of four extrinsic proteins of photosystem II from a red alga, Cyanidium caldarium, as studied by release-reconstitution experiments, *Biochemistry 37*, 2787−2793.
32. Kerfeld, C. A., and Krogmann, D. (1998) Photosynthetic cytochromes c in cyanobacteria, algae, and plants, *Annu. Rev. Plant Physiol. Plant Mol. Biol. 49*, 397−425.
33. Williams, J. G. K. (1988) Construction of specific mutations in Photosystem II photosynthetic reaction center by genetic engineering methods in Synechocystis 6803, *Methods Enzymol. 167*, 766−778.
34. Sambrook, J., Fritsch, E. F., and Maniatis, T. (1989) *Molecular Cloning: A Laboratory Manual*, 2nd ed., Cold Spring Harbor Laboratory, Cold Spring Harbor, New York.
35. Burnap, R. L., Qian, M., Shen, J. R., Inoue, Y., and Sherman, L. A. (1994) Role of disulfide linkage and putative intermolecular binding residues in the stability and binding of the extrinsic manganese stabilizing protein to the photosystem II reaction center, *Biochemistry 33*, 13712−13718.
36. Li, Z., Bricker, T. M., and Burnap, R. (2000) Kinetic characterization of His-tagged CP47 photosystem II in Synechocystis sp. PCC6803, *Biochim. Biophys. Acta 1460*, 384−389.
37. Qian, M., Dao, L., Debus, R. J., and Burnap, R. L. (1999) Impact of mutations within the putative Ca^{2+}-binding lumenal interhelical a−b loop of the photosystem II D1 protein on the kinetics of photoactivation and H_2O-oxidation in Synechocystis sp. PCC6803, *Biochemistry 38*, 6070−6081.
38. Nixon, P. J., and Diner, B. A. (1992) Aspartate 170 of the photosystem II reaction center polypeptide D1 is involved in the assembly of the oxygen evolving manganese cluster, *Biochemistry 31*, 942−948.
39. Chu, H.-A., Nguyen, A. P., and Debus, R. A. (1994) Site-directed mutagenesis of photosynthetic oxygen evolution: Instability or inefficient assembly of the manganese cluster in vivo, *Biochemistry 33*, 6137−6149.
40. Lichtenthaler, H. K. (1987) Chlorophylls and carotenoids: pigments of photosynthetic biomembranes, *Methods Enzymol. 148*, 350−382.
41. Vermaas, W. F. (1998) Gene modifications and mutation mapping to study the function of photosystem II, *Methods Enzymol. 297*, 293−310.
42. Gleiter, H. M., Haag, E., Shen, J. R., Eaton Rye, J. J., Inoue, Y., Vermaas, W. F., and Renger, G. (1994) Functional characterization of mutant strains of the cyanobacterium Synechocystis sp. PCC 6803 lacking short domains within the large, lumen exposed loop of the chlorophyll protein CP47 in photosystem II, *Biochemistry 33*, 12063−12071.
43. Qian, M., Al Khaldi, S. F., Putnam Evans, C., Bricker, T. M., and Burnap, R. L. (1997) Photoassembly of the photosystem II $(Mn)_4$ cluster in site directed mutants impaired in the binding of the manganese stabilizing protein, *Biochemistry 36*, 15244−15252.
44. Li, Z. L., and Burnap, R. L. (2001) Mutations of arginine 64 within the putative Ca(2+)-binding lumenal interhelical a−b loop of the photosystem II D1 protein disrupt binding of the manganese stabilizing protein and cytochrome *c*(550) in Synechocystis sp. PCC6803, *Biochemistry 40*, 10350−10359.
45. Philbrick, J. B., Diner, B. A., and Zilinskas, B. A. (1991) Construction and characterization of cyanobacterial mutants lacking the manganese-stabilizing polypeptide of Photosystem II. *J. Biol. Chem. 266*, 13370−13376.
46. Young, A., McChargue, M., Frankel, L. K., Bricker, T. M., and Putnam-Evans, C. (2002) Alterations of the oxygen-evolving apparatus induced by a 305Arg → 305Ser mutation in the CP43 protein of photosystem II from Synechocystis sp. PCC 6803 under chloride-limiting conditions, *Biochemistry 41*, 15747−15753.
47. Miyao, M., and Murata, N. (1985) The Cl^- effect on photosynthetic oxygen evolution: interaction of Cl^- with 18-kDa, 24-kDa and 33-kDa proteins, *FEBS Lett. 180*, 303−308.
48. Kuwabara, T., Miyao, M., Murata, T., and Murata, N. (1985) The function of the 33 kDa protein in the photosynthetic oxygen-evolution system studied by reconstitution experiments, *Biochim. Biophys. Acta 806*, 283−289.

49. Ono, T.-A., and Inoue, Y. (1983) Mn-preserving extraction of 33-, 24- and 16-kDa proteins from O_2-evolving PS II particles by divalent salt-washing, *FEBS Lett. 164*, 255−260.
50. Ono, T. A., and Inoue, Y. (1986) Effects of removal and reconstitution of the extrinsic 33-kilodalton 24-kilodalton and 16-kilodalton proteins on flash oxygen yield in photosystem ii particles, *Biochim. Biophys. Acta 850*, 380−389.
51. Bricker, T. M. (1992) Oxygen evolution in the absence of the 33-kilodalton manganese stabilizing protein, *Biochemistry 31*, 4623−4628.
52. Gleiter, H. M., Haag, E., Shen, J. R., Eaton Rye, J. J., Seeliger, A. G., Inoue, Y., Vermaas, W. F., and Renger, G. (1995) Involvement of the CP47 protein in stabilization and photoactivation of a functional water oxidizing complex in the cyanobacterium Synechocystis sp. PCC 6803, *Biochemistry 34*, 6847−6856.
53. Bouges-Bocquet, B. (1973) Limiting steps in photosystem II and water decomposition in *Chlorella* and spinach chloroplasts, *Biochim. Biophys. Acta 292*, 772−785.
54. Messinger, J., and Renger, G. (1993) Generation, oxidation by the oxidized form of the tyrosine of polypeptide D2, and possible electronic configuration of the redox states S_0, S_{-1}, S_{-2} of the water oxidase in isolated spinach thylakoids, *Biochemistry 32*, 9379−9386.
55. Vass, I., and Styring, S. (1991) pH-Dependent charge equillibria between tyrosine-D and the S-states in photosystem II. Estimation of the midpoint redox potentials, *Biochemistry 30*, 830−839.
56. Seeliger, A. G., Kurreck, J., and Renger, G. (1997) Kinetics of S2 and S3 reduction by tyrosine Y(D) and other endogenous donors as a function of temperature in spinach PS II membrane fragments with a reconstituted plastoquinone pool, *Biochemistry 36*, 2459−2464.
57. Vass, I., and Styring, S. (1994) Redox interaction of tyrosine-D with the S-states of the water-oxidizing complex in intact and chloride-depleted photosystem II, *Biochim. Biophys. Acta 1185*, 65−74.
58. Messinger, J., and Renger, G. (1994) Analyses of pH induced modifications of the period four oscillation of flash induced oxygen evolution reveal distinct structural changes of the photosystem II donor side at characteristic pH values, *Biochemistry 3327*, 10896−10905.
59. Chu, H., Hillier, W., Law, N. A., Sackett, H., Haymond, S., and Babcock, G. T. (2000) Light-induced FTIR difference spectroscopy of the S(2)-to-S(3) state transition of the oxygen-evolving complex in Photosystem II, *Biochim. Biophys. Acta 1459*, 528−532.
60. Shen, J. R., and Inoue, Y. (1993) Cellular localization of cytochrome *c*550. Its specific association with cyanobacterial photosystem II, *J. Biol. Chem. 268*, 20408−20413.
61. Barker, P. D., Nerou, E. P., Freund, S. M., and Fearnley, I. M. (1995) Conversion of cytochrome b562 to c-type cytochromes, *Biochemistry 34*, 15191−15203.
62. Barker, P. D., Nerou, E. P., Cheesman, M. R., Thomson, A. J., de Oliveira, P., and Hill, H. A. (1996) Bis-methionine ligation to heme iron in mutants of cytochrome b562. 1. Spectroscopic and electrochemical characterization of the electronic properties, *Biochemistry 35*, 13618−13626.
63. Dolla, A., Florens, L., Bianco, P., Haladjian, J., Voordouw, G., Forest, E., Wall, J., Guerlesquin, F., and Bruschi, M. (1994) Characterization and oxidoreduction properties of cytochrome *c*3 after heme axial ligand replacements, *J. Biol. Chem. 269*, 6340−6346.
64. Miles, C. S., Manson, F. D., Reid, G. A., and Chapman, S. K. (1993) Substitution of a haem-iron axial ligand in flavocytochrome b2, *Biochim. Biophys. Acta 1202*, 82−86.
65. Mus-Veteau, I., Dolla, A., Guerlesquin, F., Payan, F., Czjzek, M., Haser, R., Bianco, P., Haladjian, J., Rapp-Giles, B. J., Wall, J. D., and et al. (1992) Site-directed mutagenesis of tetraheme cytochrome *c*3. Modification of oxidoreduction potentials after heme axial ligand replacement, *J. Biol. Chem. 267*, 16851−16858.
66. Raphael, A. L., and Gray, H. B. (1989) Axial ligand replacement in horse heart cytochrome *c* by semisynthesis, *Proteins 6*, 338−340.
67. Nakai, M., Ishiwatari, H., Asada, A., Bogaki, M., Kawai, K., Tanaka, Y., and Matsubara, H. (1990) Replacement of putative axial ligands of heme iron in yeast cytochrome *c*1 by site-directed mutagenesis, *J. Biochem. 108*, 798−803.
68. Wallace, C. J., and Clark-Lewis, I. (1992) Functional role of heme ligation in cytochrome *c*. Effects of replacement of methionine 80 with natural and non-natural residues by semisynthesis, *J. Biol. Chem. 267*, 3852−3861.
69. Darrouzet, E., Mandaci, S., Li, J., Qin, H., Knaff, D. B., and Daldal, F. (1999) Substitution of the sixth axial ligand of *Rhodobacter capsulatus* cytochrome *c*1 heme yields novel cytochrome *c*1 variants with unusual properties, *Biochemistry 38*, 7908−7917.
70. Pettigrew, G. W., and Moore, G. R. (1987) *Cytochromes c: Biological Aspects*, Springer-Verlag, Berlin.
71. Vrettos, J. S., Stone, D. A., and Brudvig, G. W. (2001) Quantifying the ion selectivity of the Ca(2+) site in photosystem II: Evidence for direct involvement of Ca(2+) in O(2) formation, *Biochemistry 40*, 7937−7945.
72. Boussac, A., Rappaport, F., Carrier, P., Verbavatz, J. M., Gobin, R., Kirilovsky, D., Rutherford, A. W., and Sugiura, M. (2004) Biosynthetic Ca^{2+}/Sr^{2+} exchange in the photosystem II oxygen evolving enzyme of Thermosynechococcus elongatus, *J. Biol. Chem. 279*, 22809−22819.
73. Chu, H. A., Nguyen, A. P., and Debus, R. J. (1995) Amino acid residues that influence the binding of manganese or calcium to photosystem II. 1. The lumenal interhelical domains of the D1 polypeptide, *Biochemistry 34*, 5839−5858.
74. Ghanotakis, D. F., Babcock, G. T., and Yocum, C. F. (1984) Calcium reconstitutes high rates of oxygen evolution in polypeptide depleted photosystem II preparations, *FEBS Lett. 167*, 127−130.
75. Miyao, M., and Murata, N. (1984) Effect of urea on photosystem II particles. Evidence for an essential role of the 33 kilodalton polypeptide in photosynthetic oxygen evolution, *Biochim. Biophys. Acta 765*, 253−257.
76. Stewart, A., and Bendall, D. (1981) Properties of oxygen-evolving photosystem-II particles from Phormidium laminosum, a thermophilic blue-green alga, *Biochem. J. 194*, 877−887.
77. Satoh, K., and Katoh, S. (1985) Inhibition by ethylenediamine tetraactetate and restoration by Mn^{2+} and Ca^{2+} of oxygen-evolving activity in Photosystem II preparation from the thermophilic cyanobacterium, *Biochim. Biophys. Acta 806*, 221−229.
78. Kirilovsky, D., Boussac, A. G. P., Van, M. F. J. E., Ducruet, J. M. R. C., Stief, P. R., Yu, J., Vermaas, W. F. J., and Rutherford, A. W. (1992) Oxygen-evolving photosystem II preparation from wild type and photosystem II mutants of Synechocystis-sp PCC 6803, *Biochemistry 31*, 2099−2107.
79. Mizusawa, N., Kimura, Y., Ishii, A., Yamanari, T., Nakazawa, S., Teramoto, H., and Ono, T. A. (2004) Impact of Replacement of D1 C-terminal Alanine with Glycine on Structure and Function of Photosynthetic Oxygen-evolving Complex, *J. Biol. Chem. 279*, 29622−29627.
80. Chu, H. A., Hillier, W., and Debus, R. J. (2004) Evidence that the C-terminus of the D1 polypeptide of photosystem II is ligated to the manganese ion that undergoes oxidation during the S1 to S2 transition: an isotope-edited FTIR study, *Biochemistry 43*, 3152−3166.
81. Forbush, B., Kok, B., and McGloin, M. P. (1971) Cooperation of charges in photosynthetic O_2 evolution: II Damping of flash yield oscillation deactivation, *Photochem. Photobiol. 14*, 307−321.

BI0486738